Published in final edited form as:
J Biol Chem. 2008 March 7; 283(10): 6175–6183. doi:10.1074/jbc.M701008200.

The Endoplasmic Reticulum Exit of Glutamate Transporter Is Regulated by the Inducible Mammalian Yip6b/GTRAP3-18 Protein[*,Ⓢ]

Alicia M. Ruggiero[‡,1], **Yiting Liu**[§], **Svetlana Vidensky**[§], **Susanne Maier**[¶], **Elizabeth Jung**[§], **Hesso Farhan**[¶], **Michael B. Robinson**[‖], **Harald H. Sitte**[¶], and **Jeffrey D. Rothstein**[‡,§,2]

[‡]Department of Neuroscience, Johns Hopkins University, Baltimore, Maryland 21287

[§]Department of Neurology, Johns Hopkins University, Baltimore, Maryland 21287

[¶]Institute of Pharmacology, Center for Biomolecular Medicine and Pharmacology, Medical University of Vienna, Waehringerstrasse 13a, A-1090 Vienna

[‖]Departments of Pharmacology and Pediatrics, Children's Hospital of Philadelphia, University of Pennsylvania, Philadelphia, Pennsylvania 19104

Abstract

GTRAP3-18 interacts with and reduces the activity of the neuronal specific Na^+/K^+ glutamate transporter, EAAC1 both *in vitro* and *in vivo*. GTRAP3-18 and the related isoform, JM4, are distant relatives of the Rab GTPase-interacting factor PRA1, and share a topology of four transmembrane domains and cytosolic termini. GTRAP3-18 and JM4 are resident endoplasmic reticulum (ER) proteins. The physiological role of GTRAP3-18 is poorly understood. We demonstrate for the first time that GTRAP3-18 is a regulator of ER protein trafficking. Expression of GTRAP3-18 delays the ER exit of EAAC1, as well as other members of the excitatory amino acid transporter family. GTRAP3-18 uses hydrophobic domain interactions in the ER membrane to self-associate and cytoplasmic interactions at the C terminus to regulate trafficking. The features of GTRAP3-18 activity are consistent with recent phylogenic sequence analyses suggesting GTRAP3-18 and JM4 be reclassified as mammalian isoforms of the yeast protein family Yip, Yip6b, and Yip6a, respectively.

We identified GTRAP3-18[3] (glutamate transporter-associated protein of EAAT3), a 22-kDa protein that is dynamically induced by retinoic acid both *in vitro* and *in vivo* and inhibits the activity of EAAC1 in a dose-dependent manner (GeneID 66028) (1). EAAC1 (human

[*]This work was supported in part by National Institutes of Health NS40151 (to J. D. R.), NS36465 (to J. D. R. and M. B. R.), Austrian Science Foundation/FWF 17076 (to H. H. S.), P18076 (to S. M.), and Austrian National Bank 10507 (to H. F.).

Ⓢ The on-line version of this article (available at http://www.jbc.org) contains supplemental Fig. S1.

[2]To whom correspondence should be addressed: Dept. of Neurology, Johns Hopkins University, Meyer 6-109, 625 N. Wolfe St., Baltimore, MD 21287. Tel.: 410-614-3846; Fax: 410-955-0672; jrothstein@jhmi.edu.
[1]Present address: Vanderbilt University, Dept. of Pharmacology, Center for Molecular Neuroscience, 465 21st Ave., Nashville, TN 37232.

[3]The abbreviations used are: GTRAP3-18, glutamate transporter-associated protein of EAAT3; HA, hemagglutinin; ANOVA, analysis of variance; CFP, cyan fluorescent protein; YFP, yellow fluorescent protein; FRET, fluorescence resonance energy transfer; ER, endoplasmic reticulum; Endo H, endoglycosidase H; TMD, transmembrane domain.

Europe PMC Funders Author Manuscripts

nomenclature EAAT3) is an isoform of the plasma membrane glutamate transporter family localized to glutamatergic and GABAergic neuronal populations and is an important physiological component of normal and abnormal synaptic transmission (2–5). Antisense reduction in GTRAP3-18 or removal of the C-terminal interaction site eliminates GTRAP3-18-mediated alterations of EAAC1 activity (1). The mechanism of this activity was unknown but speculated to be related to interaction-dependent alterations to EAAC1 protein conformation or transport activity before cell surface delivery.

The expression of GTRAP3-18 has been found to be induced by diverse stimuli including oncogenic transformation and ER Ca^{2+} depletion. Chronic morphine administration leads to a 300–400% increase in GTRAP3-18 mRNA (6). Differentiation, heat shock, or oxidative stress increase the expression of the human isoform of GTRAP3-18, JWA (7, 8). These findings have been confirmed by microarray studies demonstrating increased expression of GTRAP3-18 mRNA under conditions of cell stress, inflammation, and cancer (GeoID 5194496).

Molecular modeling and reported data concur that GTRAP3-18 is an integral ER membrane protein (9) with four transmembrane domains and cytosolic N and C termini (10). GTRAP3-18 and JM4, its closest relative (39% identity 61% consensus; GeneID 11230), are structurally homologous to the Ras superfamily in their secondary structure and low molecular weight, but lack a GTP-binding consensus motif. They are conserved in human, rat, and mouse and have a homologue in *Caenorhabditis elegans* (D2096.2). Phylogenic tree analysis of these conserved gene products was used to suggest reclassification as members of the expanded mammalian Yip 6 family: GTRAP3-18/JWA as Yip6b and JM4 as Yip6a, despite an undetermined cellular function (10). The Yip family is loosely defined as integral membrane Ypt-interacting proteins, which often self-associate (11). Ypt proteins are yeast Rab GTPases (10, 12). One of the many functions assigned to Rab proteins is to regulate membrane trafficking spatially and temporally (13). Here we demonstrate that GTRAP3-18 and JM4 have a dominant effect to delay ER to Golgi trafficking.

EXPERIMENTAL PROCEDURES

Antibodies

Rabbit and chicken polyclonal anti-GTRAP3-18 antibodies were raised against peptide sequences from the N and C termini of the protein sequence: N1-GTRAP3-18: KFFPGSDRFARPDFRD,C1-GTRAP3-18: KEQQEDSINKFADYIS, and N2-GTRAP3-18: KMDVNLAPLRAWDDF; polyclonal EAAC1 antibody described previously (14, 15). Commercial antibodies included: anti-HA monoclonal and polyclonal, Giantin polyclonal, GFP and His_6 mouse monoclonal: BAbCo/Covance, anti c-Myc mouse monoclonal: Roche Applied Science, Calnexin polyclonal: Stressgen. Secondary Cy dye series (Cy2, Cy3, Cy5): Jackson Laboratories.

Plasmid Constructs

The eukaryotic expression vectors pcDNA3 and PRK5 were used for cDNA expression in the mammalian cell lines HEK 293T, COS-7 or in primary cortical neurons. GTRAP3-18

was cloned in-frame with the epitope tag HA into PRK5 using PCR-engineered Sal/Not sites. GTRAP3-18 was detectable at 23 kDa with a mouse monoclonal HA antibody (BAbCo) by Western blot analysis and corresponded to our rabbit and chicken anti-peptide polyclonal antibodies. YFP and CFP GTRAP3-18 were expressed in pEYFP-C1 and pECFP-C1 (Clontech) using PCR-engineered EcoRI/KpnI sites. EAAC1 cDNA was subcloned in myc-PRK5 to create EAAC1-myc fusion and in EcoRI/KpnI frame of pEYFP-C1 and pECFP-C1 (Clontech) using PCR-engineered restriction sites. Myc-N206S EAAT2 and full-length EAAT4 were provided by Mandy Jackson (University of Edinburgh) (16, 17). EAAT4-GFP in pEGFP was provided by Dan Gincel (Johns Hopkins). Full-length myc-GLT-1 in pCMV and hEAAT isoforms in pGBKT7 were provided by Mitsunori Watanabe (Johns Hopkins) and full-length and EAAT2 in pcDNA3.1 with the FLAG epitope was provided by Julia Fuchs (Göettingen University) following modifications (18). The GTRAP3-18 homologue, JM4 was the gift of Marc Schweneker (University of Zurich).

Yeast Two-hybrid Screen

GTRAP3-18 was cloned into pACT2 and pPC86, and the hEAAT isoforms and EAAC1 truncations were cloned in pGBKT7 and pPC97, via PCR-engineered restriction sites EcoRI and Sal1/Not1, respectively. The sequences were: E1 (462–542), E2(462–574), E3(429–525), E4(486–565). The EAAC1 C terminus was further truncated into three regions: an extracellular loop (L, amino acids 431–443) that comprises part of both the glutamate binding and ER trafficking domains (19, 20), the final transmembrane domain (T, amino acids 444–469), and the cytosolic tail (C, amino acids 470–523) (21, 22). Dual transformed yeast was selected for growth on histidine drop-out media and for β-galactosidase expression in the auxotrophic yeast strains MaV203 and AH109. Detailed results of these assays may be obtained by contacting the authors.

Mammalian Cell Transfection

HEK293 and COS-7 cell lines were maintained according to standard protocols (ATCC), split 1 day before transfection and used at 50% confluency. All mammalian cells were transfected using FuGENE 6 reagent (Roche Applied Science) according to the manufacturer's directions. Cells were harvested at 16–72 h growth according to the experimental design.

Immunohistochemistry

Cells were fixed in 4% paraformaldehyde, rinsed, solubilized in 0.4% Triton X-100 for 30 min at 4 °C, and rinsed in TBS (50 mM Tris, pH 7.4, 150 mM NaCl). Primary (Roche Applied Science) antibodies were added at final concentrations ranging from 1:200 to 1:2000. Secondary antibodies Cy2 and Cy5 anti-mouse or anti-rabbit and Cy3 anti-chicken IgY (Jackson Antibodies) were chosen by experiment. Confocal microscopy of transfected cells in brain sections, hippocampal slice, disassociated cultures, and mammalian cells was performed with a Zeiss LSM 510 laser scanning microscope.

Na^+-dependent Glutamate Uptake Assay

The activity and kinetics of expressed EAAT was assayed as described (1). Statistical analysis performed using Student's *t* test and two-way ANOVA.

Membrane Impermeant Biotinylation

Biotinylation was performed as described with some modifications (1, 17, 23). Visualized bands were analyzed and quantitated using electronic imaging and software (Versa Doc, Bio-Rad).

Enzymatic Deglycosylation

Endo H and PNGase were purchased from NEB. Cell lysates following biotinylation were digested at 37 °C for 12 h with gentle shaking with 2 units/μl of each enzyme in lysis buffer with the addition of 1% Nonidet P-40 detergent. Lysis buffer consisted of 100 mM Tris, pH 7.4, 150 mM NaCl, 1 mM EDTA, 1% Triton X-100, 0.1% SDS, and protease inhibitor mixture (Roche Applied Science). Control samples were diluted and incubated without the addition of enzyme. The biotinylation assay was then completed as described above, or the samples were diluted in 2× loading buffer and analyzed by Western blotting.

Site-directed Mutagenesis

Site-directed mutagenesis of rEAAT3 at Asn-85, -128, -178, and -197 to Gln was performed using the QuikChange Site-directed Mutagenesis kit (Stratagene) as directed by the manufacturer. Mutagenesis of Pro-118 to Gly was performed in the same manner. Clones were verified by sequence analysis.

Metabolic Labeling

Metabolic labeling of HEK293T cells was performed as described (24). The cells were transfected with Myc-rEAAC1 and HA-GTRAP3-18 at a 1:2 or a 1:1 ratio and pulsed with Trans-Label (ICN) at 3.5 h post-transfection for 10 min followed by media chase for up to 16 h. Harvested cells were lysed and immunoprecipitated with c-Myc as described. Bound proteins were eluted and analyzed by SDS-PAGE and ^{35}S emission on film.

FRET Analysis

Two methods were used to detect FRET: donor recovery after acceptor photobleaching (DRAP (27); and the three-filter method according to Youvan (19), (28). The equipment used consisted of an epi-fluorescence microscope (Carl Zeiss TM210, Germany) COS7 cells (3×10^5/well); images were taken using a ×63 oil objective and a LUDL filter wheel that allows for rapid exchange of filters (less than 100 ms). The system was equipped with the following fluorescence filters: CFP filter (I_{CFP}; exc.: 436 nm, dichr.: 455 nm, em.: 480 nm), YFP filter (I_{YFP}; exc.: 500 nm, dichr.: 515 nm, em.: 535 nm), and FRET filter (I_{FRET}: excitation = 436 nm, dichroic mirror = 455 nm, emission = 535 nm). The acquisition of the images was performed with MetaMorph software (Meta Imaging, Universal Imaging Corporation, V. 4.6.).

HEK293 cells were seeded on to poly-D-lysine-coated glass coverslips (24-mm diameter). The next day, cells were transiently transfected using the calcium phosphate precipitation method: 1–3 μg of cDNA was mixed with $CaCl_2$ and HBS buffer (280 mM NaCl/10 mM KCl/1,5 mM Na_2HPO_4/12 mM dextrose/50 mM HEPES); after 6–10 min, the calcium phosphate-DNA precipitate was added to the cells. After 4–5 h, the cells were washed twice with phosphate-buffered saline and briefly treated with glycerol, followed by the addition of fetal calf serum-containing medium. Media were replaced by Krebs-HBS buffer (10 mM HEPES, 120 mM NaCl, 3 mM KCl, 2 mM $CaCl_2$, 2 mM $MgCl_2$). For DRAP, a CFP image was acquired before (Ib) and after (Ia) photo-bleaching using the YFP filter settings for 90 s. DRAP in a specific region of interest (intracellular parts that mostly show red to white color in the representative image) was quantified by FRET efficiency (E) as described in (24) according to Equation 1.

$$\mathrm{E} = (\mathrm{Ia} - \mathrm{Ib}) / \mathrm{Ia} \quad \text{(Eq.1)}$$

Images for the three-filter method were taken using a double dichroic mirror for all measurements. Various combinations of excitation and emission filters were used to produce the CFP, YFP, and FRET images (ICFP, IYFP, and IFRET, respectively). Background fluorescence was subtracted from all images; net FRET (nF) was calculated using Equation 2,

$$\mathrm{nF} = \mathrm{IFRET} - (\alpha \times \mathrm{IYFP}) - (\beta \times \mathrm{ICFP}) \quad \text{(Eq.2)}$$

where α and β represent the bleed-through values for YFP (0.319 ± 0.001; n = 15) and for CFP (0.656 ± 0.006; n = 14). To gauge the system both with positive and negative controls for FRET imaging, we used a fusion protein of CFP and YFP (termed CYFP; Ref. 25) and the CFP-tagged deletion mutant of the rat GABA transporter 1, CFP-rGAT1Δ37, lacking the last 37 amino acids, respectively.

Statistical Analysis

Statistical analysis was performed using Student's *t* test and two-way ANOVA for all *n*. All experiments were performed with a minimum n = 3 replicates.

RESULTS

GTRAP3-18 Prevents Complex Oligosaccharide Formation on EAAC1 in a Dose-dependent Manner

EAAC1 and all members of the EAAT/ASCT gene family are *N*-linked (asparagine) glycosylated (26). The *N*-linked oligosaccharides are processed to the complex state by resident Golgi enzymes preceding cell surface delivery (27). Therefore, the state of the oligosaccharide may be used as an indicator of the extent of ER-Golgi trafficking and plasma membrane localization (27). EAAC1 expressed in mixed cortical cultures (Fig. 1*A*, *lane 1*) was separated into intracellular (*lane 2*) and plasma membrane (*lane 3*) pools using membrane-impermeant biotinylation (n = 3). EAAC1 predominantly resides in intracellular compartments (*lane 2*) (28). The cell surface population of EAAC1 (*lane 3*) is enriched for complex oligosaccharide EAAC1 (70 kDa) (27). EAAC1 protein forms a homotrimeric

complex that is not completely disrupted by SDS-PAGE analysis (29). The visualization of these dimeric and trimeric protein bands in Western analysis are typical of all molecular subtypes of plasma membrane glutamate transporters (14).

We verified the assigned glycosylation state of EAAC1 protein using endoglycosidase treatment. The cortical culture cell lysates were exposed to the following treatments: no endoglycosidase (Fig. 1*B*, *lane 1*), Endo H (*lane 2*), or PNGase F (*lane 3*) ($n = 3$). Endo H selectively digests high mannose *N*-linked oligosaccharides. High mannose oligosaccharides are processed by enzymes resident in the Golgi; therefore, the presence of a high mannose oligosaccharide indicates that the protein has not left the ER membrane following translation. The endoglycosidase PNGase F, cleaves all *N*-linked oligosaccharides. The processed state of the oligosaccharide is noted by *arrows*; complex state (70 kDa) EAAC1 is Endo H-insensitive (*black arrow*), but the high mannose EAAC1 (60 kDa) is reduced by Endo H (*lane 2*, *gray arrow*). All oligosaccharides are cleaved by PNGase F, resulting in immunoreactive band collapse to 50 kDa (*lane 3*). We utilize endoglycosidase digest analysis in subsequent figures.

The expression of GTRAP3-18 is inducible and is maintained at very low levels in native tissue (1). In Fig. 1*C*, lysates of HEK 293T cells and adult mouse brain (20 μg per lane) are compared with that of HEK-293T cells transfected with GTRAP3-18 cDNA. The expression level of transfected GTRAP3-18 is comparable to that found in brain tissue lysate (Fig. 1*C*, *lanes 2–3*). The endogenous level of GTRAP3-18 is difficult to detect in mammalian cell lines (Fig. 1*C*, *lane 1*). We are unable to detect endogenous expression of GTRAP3-18 in multiple cell lines by Western blot analysis using 60 μg of cell lysate (data not shown). Mouse GTRAP3-18 is 97.9% identical to rat GTRAP3-18. The peptide sequence used to generate the antibody corresponds to a fully conserved region. However at the low molecular weight this subtle difference creates a band shift on Western blot analysis. We have found GTRAP3-18 expression to be potent and dose-dependent at this level of transfected expression (see Fig. 1*G*). The analysis of GTRAP3-18 presented here was performed using transfected GTRAP3-18 cDNA in mammalian cell lines at levels of expression that mimic the expression found in adult brain tissue from mouse or rat.

We generated epitope-tagged cDNA constructs of GTRAP3-18 and EAAC1 to facilitate our analysis of the protein interaction. The addition of these small N-terminal epitope tags did not interfere with the expression, trafficking, or activity of the proteins (data not shown). In our initial characterization of GTRAP3-18 the mechanism by which GTRAP3-18-mediated decrease in EAAC1 cell surface activity was not described (1). Endoglycosidase digestion reveals that the processing of EAAC1 oligosaccharide chains is reduced following GTRAP3-18 co-expression (Fig. 1*D*, compare *lanes 1–3* with *4–6*) ($n = 6$). The EAAC1 cell lysate (*lane 1*) is only partially sensitive to Endo H (*lane 2*). The EAAC1 and GTRAP3-18 cotransfected cell lysate (*lane 4*) has an increased sensitivity to Endo H digestion (*lane 5*). GTRAP3-18 expression leads to enrichment of the high mannose EAAC1 and a reduction in complex oligosaccharide EAAC1 populations (*see arrows*).

Alterations in oligosaccharide processing that reduce the complex oligosaccharide form of EAAC1 correspond with a decrease in cell surface expression. Both oligosaccharide species

of EAAC1 are evident in the whole cell lysate (Fig. 1*E*, *lanes 1–3*, see *arrows*) ($n = 8$), but it is the complex oligosaccharide form of EAAC1 that is associated with plasma membrane localization (*lane 3*). Following GTRAP3-18 co-transfection the amount of high mannose oligosaccharide EAAC1 is increased and there is a decrease in the amount of complex oligosaccharide EAAC1 in the lysate (Fig. 1*E*, *lanes 3–6;* see *arrows*) leading to a decrease in cell surface expression (*lane 6*). This newly recognized physiological effect of GTRAP3-18 on the oligosaccharide maturation of EAAC1 suggests that GTRAP3-18 is involved in the trafficking of EAAC1 and that GTRAP3-18 is functioning in the ER. The reduction of ER-Golgi trafficking of EAAC1 is associated with a concomitant reduction in plasma membrane Na^+-dependent glutamate uptake activity of EAAC1 following co-transfection with GTRAP3-18 (Fig. 1*F*, $p < 0.001$) as previously described (1).

Our initial characterization of GTRAP3-18 found its activity on EAAC1 to be dose-dependent (1). This dose dependence correlates with the physiological effect of GTRAP3-18 to prevent ER to Golgi trafficking of greater percentages of the EAAC1 protein, thereby limiting cell surface expression (Fig. 1*G*). As the GTRAP3-18 co-transfection is increased 2-fold (*lanes 4–6* and *7–9*), the level of complex oligosaccharide cell surface-expressed EAAC1 is decreased (*lanes 3*, *6*, and *9*). JM4, the GTRAP3-18 homologue, has similar capabilities in regulating EAAC1 trafficking (*lanes 10–12*) and is also localized to the ER (data not shown).

GTRAP3-18 Activity Requires Four α-Helical Transmembrane Domains and Homo-oligomerization

The *α*-helical domains of GTRAP3-18 self-associate and GTRAP3-18 activity may be reconstituted by this association. We generated multiple truncations of GTRAP3-18 to determine domains important for activity (truncations diagrammed in supplemental Fig. S1). GTRAP3-18 protein has four transmembrane domains and cytosolic termini. The symmetrical GTRAP3-18 truncations, N-2TMD (transmembrane domains) (amino acids 1–93), and C-2TMD (amino acids 94–188), each have one cytosolic tail and two *α*-helical transmembrane domains. Following co-transfection (Fig. 2*A*), these truncated proteins are unable to alter the extent of plasma membrane expression of EAAC1 (*lanes 6* and *8*) or the ratio of high mannose to complex EAAC1 oligosaccharide (*see arrows*) ($n = 5$). They are also unable to reduce the Na^+-dependent glutamate uptake activity of EAAC1 (data not shown). However, these truncated GTRAP3-18 proteins retain ER localization (data not shown). The trafficking activity of the N-2TMD and C-2TMD is reconstituted by co-transfection of both fragments (*lanes 9–10*). This reconstitution of GTRAP3-18 activity in the ER suggests that the *α*-helical transmembrane domains of GTRAP3-18 self-oligomerize in the ER membrane and that oligomerization is required for the prevention of ER to Golgi trafficking. The self-oligomerization of *α*-helical domains has been proposed as a means to enhance activity and selectivity for the Yip family, the GTRAP3-18 protein family in yeast, and has been demonstrated for PRA1/Yip3 (10, 30). EAAC1 expression (*lanes 1–2*) and EAAC1 co-transfected with full-length GTRAP3-18 (*lanes 3–4*) is shown for comparison and demonstrates the loss of complex oligosaccharide and membrane expression. The expression of GTRAP3-18 truncations is shown by anti-HA Western analysis and equal protein loading is verified by Western analysis of the transferrin receptor (TFR).

We conducted two complementary FRET microscopy methods to address the homo-association properties of GTRAP3-18: donor recovery after acceptor photobleaching (DRAP) FRET microscopy and the three filter method. DRAP FRET relies on the premise that the donor fluorescence increases after complete photobleaching of the acceptor; this occurs only when energy transfer from a donor to acceptor fluorophore occurs. In Fig. 2*B*, significant GTRAP3-18 self-association in the ER is measured by DRAP FRET analysis of CFP- and YFP-tagged forms GTRAP3-18 (25). We transfected HEK293 cells with the following control plasmids to gauge our system, cyan fluorescent protein (CFP)-tagged mutant form of the GABA transporter 1 (GATΔ37) that strictly resides in the ER as negative control, and a concatemeric form of CFP and YFP termed CYFP (25) that shows strong energy transfer upon excitation as shown in Fig. 2*C*. A summary of 6 experimental days with 6–10 values each (Fig. 2*C*, shown as means ± S.E.) are shown and the DRAP-FRET efficiency (E) was calculated as described under "Experimental Procedures." When we co-transfected the CFP- and YFP-tagged forms of EAAC1, the value was indicative of homo-oligomerization between these subunits, in agreement with the observations by Gouaux' group (29). Similar results have been obtained upon application of the three filter method (data not shown).

Are α-helical domains of GTRAP3-18 solely mediating activity? What is the relative contribution of the cytosolic N- and C-terminal sequence of GTRAP3-18? Deletion of either or both of the GTRAP3-18 cytosolic tails created the following truncated proteins: N- and TMD (amino acids 1–142), C- and TMD (amino acids 36–188), and TMD (amino acids 36–142) GTRAP3-18 (supplemental Fig. S1). In Fig. 2*D*, the N- and TMD GTRAP3-18 truncation is inactive and co-transfection with EAAC1 does not result in a loss of cell surface expression (*lanes 3–4*) ($n = 4$). However the C- and TMD (*lanes 5–6*) or TMD ((*lanes 7–8*) GTRAP3-18 truncated proteins both retain the activity to prevent ER-Golgi trafficking of EAAC1. The level of complex oligosaccharide EAAC1 (*see arrows*) and the level of cell surface expression is reduced following their co-transfection. The membrane expression of EAAC1 is shown for comparison (*lane 2*) and the transferrin receptor is shown as a control.

Following transfection, the truncated GTRAP3-18 proteins exhibit varied stability in the ER. The construct N- and TMD and full-length GTRAP3-18 accumulate to a much greater extent than the truncations C- and TMD and TMD (see HA bands). However, even at much higher protein levels the N- and TMD truncation is not active while the latter are. These data suggest that the activity of GTRAP3-18 uses signaling coordinated by both its N and C terminus. These sequences may be antagonistic in their roles to prevent the ER exit of associated EAAC1 protein.

GTRAP3-18 Is an Integral Membrane ER Protein, the Expression of Which Leads to ER Retention of EAAC1

Immunocytochemical analysis of the subcellular co-localization of GTRAP3-18 and EAAC1 is presented in Fig. 3 ($n = 4$). EAAC1 has a punctate pattern throughout the cell (Fig. 3*A*, *panel 1*, *red*), and inhabits multiple compartments of the endocytic secretory system (21,

23). The integral ER protein calnexin (*panel 2*, *blue*) is a defined ER marker (31) and co-localizes with EAAC1 in perinuclear ER structures (*panel 3*, *overlay*).

GTRAP3-18 (*panel 4*, *green*) displays a very typical ER expression pattern of tubular structures, and co-localizes extensively with calnexin, (*panel 6*, *overlay*) and other ER markers, such as the luminal ER chaperone, BiP (data not shown). GTRAP3-18 co-transfection (*panels 4–7*) delays the ER exit and delivery to the Golgi organelle of EAAC1, and the ER organelle appears enlarged. The number of EAAC1 puncta is reduced and the co-localization of EAAC1 (*panel 5*) with GTRAP3-18 and calnexin (*panel 6*) is increased. These data were obtained using COS-7 cells; the same results were found using HEK293 cells and transfected cortical neuronal cultures (data not shown).

The Golgi organelle is defined by immunofluorescent labeling of the integral membrane protein, giantin (Fig. 3*B*, *panel 2*, *blue*) ($n = 3$). The perinuclear stacked layers have some co-localization with Golgi localized EAAC1 (*panel 3*, *overlay*). Although GTRAP3-18 causes the Golgi to appear more compact (*panels 2 versus 6*), GTRAP3-18 does not co-localize with giantin (*panels 4 and 6*). The level of EAAC1 co-localization with giantin is decreased following GTRAP3-18 co-transfection (*panels 3 and 7*). It should be noted that overexpression of GTRAP3-18 resulted in a significant change in cell morphology, probably resulting from a general ER exit block or induction of ER response. This alteration is often observed following the expression of a protein involved in regulating ER to Golgi trafficking (32). These observations are in agreement with the biochemical data (Figs. 1 and 2). Additional analysis found GTRAP3-18 is not localized to proteosomes or lysosomes and GTRAP3-18 expression reduced the trafficking and distribution of EAAC1 to these two organelles (data not shown, $n = 3$). The morphology of the lysosome and proteasome organelles was not altered following GTRAP3-18 co-transfection (data not shown). These data suggest that GTRAP3-18 expression may control the ER exit of EAAC1.

GTRAP3-18 Expression Delays the High Mannose to Complex Oligosaccharide Transition of EAAC1

GTRAP3-18 co-transfection with EAAC1 inhibits ER to Golgi trafficking; do these trafficking changes alter EAAC1 protein stability? Metabolic labeling studies of EAAC1 have concluded that within 45 min of translation in mammalian cell culture, the *N*-linked oligosaccharide is processed to the complex state (27). We investigated the effects of GTRAP3-18 co-transfection on the oligosaccharide maturation of EAAC1 (Fig. 4, *A* and *B*) ($n = 4$). EAAC1 is in both high mannose and complex oligosaccharide states 30 min following ^{35}S incorporation (Fig. 4*A*, see *arrows* and *boxed lanes*). The ratio of complex oligosaccharide EAAC1 increases with time and predominates within the hours following the metabolic labeling pulse (Fig. 4*A*). Co-transfection with GTRAP3-18 delays the rapid trafficking of EAAC1 from the ER to the Golgi (Fig. 4*B*, see *arrows* and *boxed lanes*) thereby preventing the increase in the ratio of complex oligosaccharide EAAC1 on the same time scale. However, the EAAC1 protein delayed by GTRAP3-18 is able to reach the Golgi on a longer time scale of 8–12 h (*data not shown*). These data suggest GTRAP3-18 expression is able to alter intracellular trafficking events and thereby delay oligosaccharide processing.

GTRAP3-18 Restricts the ER Exit of Other Members of the Excitatory Amino Acid Transporter Family

We previously reported that the inhibitory effect of GTRAP3-18 on the neuronal glutamate transporter EAAC1 (1). Here, we tested GTRAP3-18 activity with other members of the excitatory amino acid transporter family. As seen in Fig. 5, a significant reduction in Na^+-dependent glutamate uptake activity following GTRAP3-18 co-transfection was found for, EAAT4 (5A), EAAT2 (5B), and EAAT1 (5C) ($n = 3$). Kinetic analysis of the effect of GTRAP3-18 is measured predominately as a change in V_{max} (Table 1 analysis of EAAC1 and GLT-1). The activity of GTRAP3-18 on the EAAT family was found to be through a similar mechanism as for EAAC1 (data not shown). The glutamate transporter EAAT4 is illustrative of immunocytochemical findings (Fig. 5*D*, $n = 4$). EAAT4 is preferentially expressed on the cell surface and in recycling endosomes (*panel 2, green*). A small percentage of EAAT4 co-localizes with the ER marker calnexin (*panels 1* and *3, red*); GTRAP3-18 co-transfection (*panel 4, blue*) drastically alters EAAT4 subcellular distribution to the ER (*panel 6*) and leads to extensive co-localization with calnexin (*panel 7, overlay*).

DISCUSSION

Our group identified GTRAP3-18, a protein that is dynamically induced by retinoic acid both *in vitro* and *in vivo* and inhibits the activity of EAAC1 in a dose dependent manner (1). The mechanism by which GTRAP3-18 regulated EAAC1 activity and its basic cellular properties were not initially clear. In this report, we demonstrate that GTRAP3-18 is an integral ER membrane protein, and when it is co-expressed in heterologous cells, it is able to delay the ER to Golgi trafficking of EAAC1 and other members of the excitatory amino acid transporter family. Considering the localization of GTRAP3-18 in the ER, at the early stage of the protein trafficking, it is possible that the ER exit of other cell surface transporters or receptors may be regulated by GTRAP3-18. Besides the EAAT family members, our preliminary data show that GTRAP3-18 has the ability to regulate the trafficking of selected additional neuron-transmitter transporters and receptors. For example, the Na^+/Cl^- family of neurotransmitter transporters are not well conserved with the EAAT family at the sequence level, but do share aspects of channel and transport function and a conserved oligomerized quaternary structure. They are predicted to have 12 transmembrane domains and form homo-oligomers of undetermined stoichiometry (33). Examples include the dopamine transporter (DAT) and the GABA transporter (GAT-1). GTRAP3-18 is able to delay the ER exit of these two proteins. The family of GPCR (G-protein-coupled receptors) is not structurally or functionally similar to transporter proteins. They have seven transmembrane domains and are heavily glycosylated (34). We examined trafficking of the β_2-AR (adrenergic receptor), $\alpha_1\beta$ receptor, and the D_2R (dopamine receptor) of this family with GTRAP3-18 co-expression. As observed for transporter family members, GTRAP3-18 increases the population of high mannose oligosaccharide state of these proteins and restricts their subcellular localization to the ER. The common feature of these cell surface transporters and G-protein-coupled receptors is that they form oligomeric complex before exit out of the ER. In contrast, GTRAP3-18 was unable to clearly alter the cell surface

expression of the plasma membrane proteins that do not oligomerize in the ER include the EGF receptor (EGFR) and SNAP-25.[4]

GTRAP3-18 utilizes hydrophobic α-helical interactions and weak oligomerization forces to function in the ER (35). The oligomerization of the four transmembrane domains of GTRAP3-18 is necessary for its activity (Fig. 2*A*). GTRAP3-18 molecules also self-associate, most likely via the hydrophobic α-helical domains. Their intramolecular oligomerization is measurable by FRET analysis (Fig. 2, *B* and *C*). The homo-oligomerization of GTRAP3-18 molecules may enhance its activity and specificity to certain oligomeric protein complexes (30, 36). The hydrophobic surface interactions between GTRAP3-18 and the oligomeric protein complexes may prevent these cargo proteins exiting out of the ER.

GTRAP3-18 and its homolog, JM4, arose as part of the expansion of Yip (yeast Rab GTPases Ypt-interacting proteins) family in mammals. This protein family emerged as strong candidates for GDFs (GDI-displacement factor), because at lease one Yip protein Yip3/PRA1 can quantitatively dissociated prenylated-Rab9-GDI complexes and recruit Rab9 onto specific membrane locations. In mammals, a protein that is related to Yip3/PRA1 has been named Yip6/PRA2. Using this nomenclature, GTRAP3-18 would be classified as Yip6b and JM4 as Yip6a (12).

The expression of GTRAP3-18 is low but has been found to be induced by stressful physiologic stimuli such as calcium depletion, oncogenic transformation, nitric-oxide synthase induction and drug withdrawal (6–8, 32, 38). What is the physiological consequence of this injury induced overexpression of GTRAP3-18 and how does it alter ER exit of EAAC1 (and other proteins)? One possible mechanism underlying the inhibitory effect of overexpressed GTRAP3-18 on the ER exit of amino acid transporters could be that increased amount of GTRAP3-18 on the ER membrane locks Rab on the membrane and in turn disrupts its distribution between cytosolic pools (GDI-bound) and membrane pools. Eventually, this blocks protein trafficking out of the ER and results in the delayed ER exit of multiple proteins as we observed. Another possibility could be that increased level of GTRAP3-18 triggers ER stress responses, such as UPR (unfolded protein response), which limits ER to Golgi trafficking (39, 40). However, the inhibitory effect of overexpressed GTRAP3-18 is not universal and appears to be restricted to certain proteins that form oligomeric complexes in the ER, suggesting a specific cargo selection and package mechanism for the oligomeric protein complexes.

Supplementary Material

Refer to Web version on PubMed Central for supplementary material.

[4]J. D. Rothstein, unpublished observations.

Acknowledgments

We thank Mandy Jackson, Margaret Dykes-Hoberg, Mitsunori Watanabe, Julia Fuchs, and Qiao Han for helpful guidance and suggestions. Randy Blakely, Haley Melikian, Gonzalo Torres, Marc Caron, and Avto Kalandadze provided reagents and critical review.

REFERENCES

1. Lin CI, Orlov I, Ruggiero AM, Dykes-Hoberg M, Lee A, Jackson M, Rothstein JD. Nature. 2001; 410:84–88. [PubMed: 11242046]
2. Diamond JS. J. Neurosci. 2001; 21:8328–8338. [PubMed: 11606620]
3. Danbolt, NC. 2001. p. 1-105. 65
4. Sepkuty JP, Cohen AS, Eccles C, Rafiq A, Behar K, Ganel R, Coulter DA, Rothstein JD. J. Neurosci. 2002; 22:6372–6379. [PubMed: 12151515]
5. Mathews GC, Diamond JS. J. Neurosci. 2003; 23:2040–2048. [PubMed: 12657662]
6. Ikemoto MJ, Inoue K, Akiduki S, Osugi T, Imamura T, Ishida N, Ohtomi M. Neuroreport. 2002; 13:2079–2084. [PubMed: 12438930]
7. Mao WG, Li AP, Ye J, Huang S, Li AQ, Zhou JW. Zhonghua Lao Dong Wei Sheng Zhi Ye Bing Za Zhi. 2004; 22:60–63. [PubMed: 15033023]
8. Wang NP, Zhou JW, Li AP, Cao HX, Wang XR. Zhonghua Lao Dong Wei Sheng Zhi Ye Bing Za Zhi. 2003; 21:212–215. [PubMed: 14761492]
9. Abdul-Ghani M, Gougeon P-Y, Prosser DC, Da-Silva LF, Ngsee JK. J. Biol. Chem. 2001; 276:6225–6233. [PubMed: 11096102]
10. Pfeffer S, Aivazian D. Nat. Rev. Mol. Cell Biol. 2004; 5:886–896. [PubMed: 15520808]
11. Calero M, Collins RN. Biochem. Biophys. Res. Commun. 2002; 290:676–681. [PubMed: 11785952]
12. Pfeffer SR. J. Biol. Chem. 2005; 280:15485–15488. [PubMed: 15746102]
13. Collins RN. Mol. Membr. Biol. 2003; 20:105–115. [PubMed: 12851068]
14. Rothstein JD, Martin L, Levey AI, Dykes-Hoberg M, Jin L, Wu D, Nash N, Kuncl RW. Neuron. 1994; 13:713–725. [PubMed: 7917301]
15. Rothstein JD, Dykes-Hoberg M, Corson LB, Becker M, Cleveland DW, Price DL, Culotta VC, Wong PC. J. Neurochem. 1999; 72:422–429. [PubMed: 9886096]
16. Trotti D, Aoki M, Pasinelli P, Berger UV, Danbolt NC, Brown RH Jr. Hediger MA. J. Biol. Chem. 2001; 276:576–582. [PubMed: 11031254]
17. Jackson M, Song W, Liu MY, Jin L, Dykes-Hoberg M, Lin CI, Bowers WJ, Federoff HJ, Sternweis PC, Rothstein JD. Nature. 2001; 410:89–93. [PubMed: 11242047]
18. Lin CL, Bristol LA, Jin L, Dykes-Hoberg M, Crawford T, Clawson L, Rothstein JD. Neuron. 1998; 20:589–602. [PubMed: 9539131]
19. Kalandadze A, Wu Y, Fournier K, Robinson MB. J. Neurosci. 2004; 24:5183–5192. [PubMed: 15175388]
20. Seal RP, Shigeri Y, Eliasof S, Leighton BH, Amara SG. Proc. Natl. Acad. Sci. U. S. A. 2001; 98:15324–15329. [PubMed: 11752470]
21. Cheng C, Glover G, Banker G, Amara SG. J. Neurosci. 2002; 22:10643–10652. [PubMed: 12486157]
22. Gonzalez MI, Bannerman PG, Robinson MB. J. Neurosci. 2003; 23:5589–5593. [PubMed: 12843260]
23. Davis KE, Straff DJ, Weinstein EA, Bannerman PG, Correale DM, Rothstein JD, Robinson MB. J. Neurosci. 1998; 18:2475–2485. [PubMed: 9502808]
24. Melikian HE, Ramamoorthy S, Tate CG, Blakely RD. Mol. Pharmacol. 1996; 50:266–276. [PubMed: 8700133]
25. Schmid JA, Scholze P, Kudlacek O, Freissmuth M, Singer EA, Sitte HH. J. Biol. Chem. 2001; 276:3805–3810. [PubMed: 11071889]

26. Arriza JL, Fairman WA, Wadiche JI, Murdoch GH, Kavanaugh MP, Amara SG. J. Neurosci. 1994; 14:5559–5569. [PubMed: 7521911]
27. Yang W, Kilberg MS. J. Biol. Chem. 2002; 31:31.
28. Dowd LA, Robinson MB. J. Neurochem. 1996; 67:508–516. [PubMed: 8764574]
29. Yernool D, Boudker O, Jin Y, Gouaux E. Nature. 2004; 431:811–818. [PubMed: 15483603]
30. Sivars U, Aivazian D, Pfeffer SR. Nature. 2003; 425:856–859. [PubMed: 14574414]
31. Trombetta ES. Glycobiology. 2003; 13:77R–91R.
32. Ward TH, Polishchuk RS, Caplan S, Hirschberg K, Lippincott-Schwartz J. J. Cell Biol. 2001; 155:557–570. [PubMed: 11706049]
33. Sitte HH, Farhan H, Javitch JA. Mol. Interventions. 2004; 4:38–47.
34. Lee SP, O'Dowd BF, George SR. Life Sci. 2003; 74:173–180. [PubMed: 14607244]
35. Teasdale RD, Jackson MR. Annu. Rev. Cell Dev. Biol. 1996; 1996:27–54. [PubMed: 8970721]
36. Pfeffer S. Biochem. Soc. Trans. 2005; 33:627–630. [PubMed: 16042559]
37. Deleted in proof
38. Li H, Gu X, Dawson VL, Dawson TM. Proc. Natl. Acad. Sci. U. S. A. 2004; 101:647–652. [PubMed: 14701905]
39. Patil C, Walter P. Curr. Opin. Cell Biol. 2001; 13:349–355. [PubMed: 11343907]
40. Rutkowski DT, Kaufman RJ. Trends Cell Biol. 2004; 14:20–28. [PubMed: 14729177]

Europe PMC Funders Author Manuscripts

Europe PMC Funders Author Manuscripts

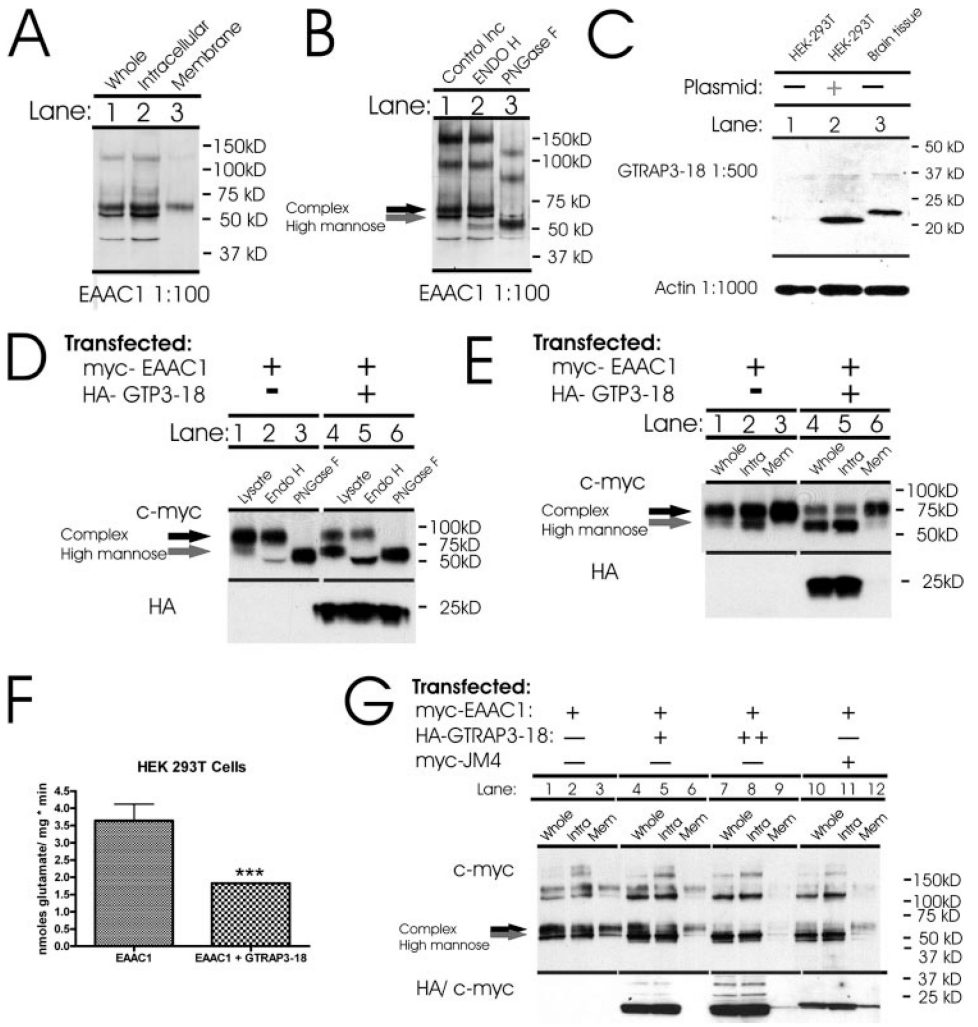

FIGURE 1. EAAC1, co-transfected with GTRAP3-18, is predominantly in the high mannose oligosaccharide form

The activity of GTRAP3-18 is dose-dependent. *A*, oligosaccharide processing of EAAC1 (*A* and *B*) is conserved between mixed cortical cultures and mammalian expression systems. The 70-kDa form is trafficked to the cell surface (*A*, *lane 3*). Endoglycosidase digestion of the cell lysates (*B*) verifies that the 70-kDa EAAC1 is resistant to Endo H, and is in the complex oligosaccharide state. The 60-kDa EAAC1 is sensitive to Endo H and is in the high mannose oligosaccharide state (*B*, *lanes 2–3*, see *arrows*). *C*, GTRAP3-18 is not detectable in mammalian cell lines (*lane 1*) and is expressed at a low level in mouse cortical tissue (*lane 3*). Transfection of GTRAP3-18 into mammalian cell lines reconstitutes a level of protein expression found in mouse cortical tissue (*lane 2*). This level of transfected expression is fairly low, and we have found GTRAP3-18 expression to be potent and dose-dependent at this level of transfected expression. *D*, EAAC1 co-transfected with GTRAP3-18 is enriched in high mannose oligosaccharide. The EAAC1 cell lysate (*D*, *lanes 1–3*), has a minor Endo H-sensitive portion (*lane 2*) and is sensitive to PNGase F (*lane 3*). The majority of EAAC1 is complex oligosaccharide. In the co-transfected EAAC1 and GTRAP3-18 cell lysate (*lanes 4–6*), all the EAAC1 protein is sensitive to both Endo H (*lane*

Europe PMC Funders Author Manuscripts

2) and PNGase F (*lane 3*), as EAAC1 is predominately high mannose oligosaccharide. *E*, plasma membrane expression of transfected EAAC1 is isolated into intracellular (*E*, *lane 2*) and plasma membrane localized (*lane 3*) fractions, and the total cell lysate is shown (*lane 1*). EAAC1 co-transfected with GTRAP3-18 (*lanes 4–6*) demonstrates a bias in the ratio of EAAC1 protein in the high mannose state (see *arrows*) with a reduction in the amount of EAAC1 on the plasma membrane (*lane 6*). Western blot analysis was performed using c-Myc and HA monoclonal and EAAC1 polyclonal antibodies. *F*, full-length GTRAP3-18 co-transfection significantly reduces the Na^+-dependent glutamate uptake activity of EAAC1 ($p < 0.001$). *G*, co-transfection of EAAC1 with a 1× molar ratio of GTRAP3-18 (*lanes 4–6*) decreases expression of the complex oligosaccharide form (see *arrows*) and reduces cell surface expression (*lane 6*) compared with EAAC1 (*lanes 1–3*). Co-expression with 2× molar ratio of GTRAP3-18 (*lanes 7–9*) further decreases the level of the complex oligosaccharide (see *arrows*) and cell surface expression (*lane 9*). The GTRAP3-18 homologue, JM4 (*lanes 10–12*), has similar activity on glycosylation (*see arrows*) and cell surface expression (*lane 12*).

Europe PMC Funders Author Manuscripts

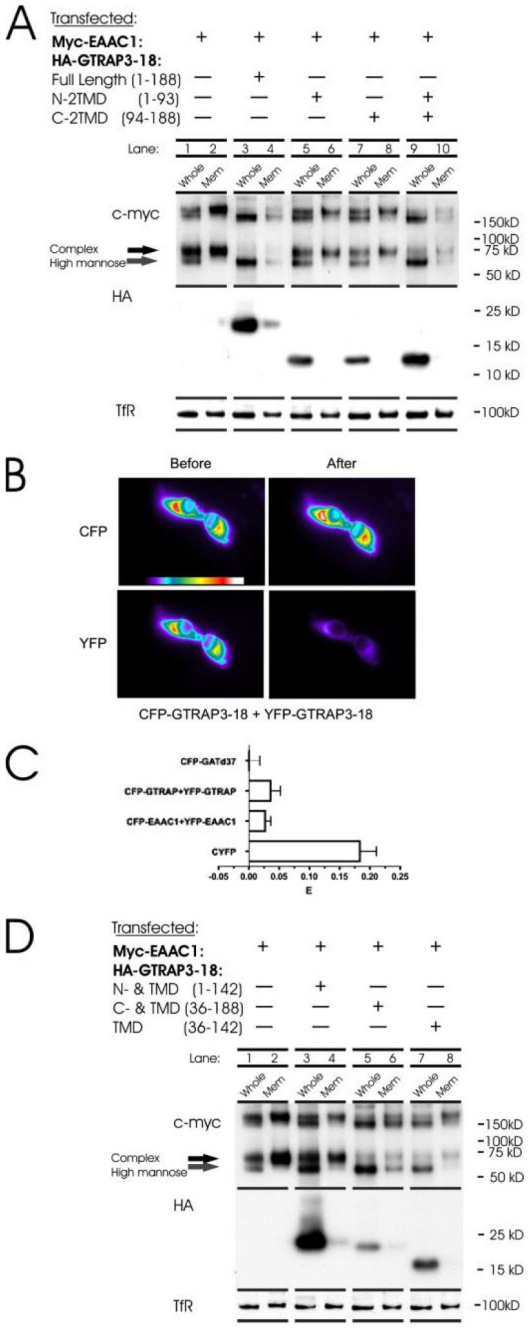

FIGURE 2. The *α*-helical domains of GTRAP3-18 self-associate and mediate activity

A, GTRAP3-18 protein has four ER transmembrane domains with cytosolic termini (see diagram in supplemental Fig. S1). A truncation of GTRAP3-18 at its center point produces the proteins, N-2TMD (amino acids 1–93) and C-2TMD (amino acids 94–188). EAAC1 (*lanes 1–2*) and the co-transfection of full-length GTRAP3-18 with EAAC1 (*lanes 3* and *4*) demonstrates the GTRAP3-18 induced reduction in complex oligosaccharide (see *arrows*) and cell surface expression (*lane 4*). The co-transfection of either N-2TMD (*lanes 4–6*, or C-2TMD (*lanes 7–8*) GTRAP3-18 with EAAC1 does not alter oligosaccharide maturation or

cell surface expression of the transporter. Co-transfection of both N-2TMD and C-2TMD reconstitutes GTRAP3-18 protein activity in the ER membrane as shown by a loss of complex oligosaccharide EAAC1 (see *arrows*) and cell surface expression (*lane 10*). *B*, GTRAP3-18 α-helical domain oligomerization in the ER membrane is measured by FRET analysis. *C*, summary of six experimental days with 6–10 values each is represented (shown as means ± S.E.). DRAP-FRET efficiency (*E*) was calculated as given under "Experimental Procedures." *D*, deletion of either or both of the GTRAP3-18 cytosolic tails result in the following truncated proteins; C- and TMD (*amino acids 36–188*), N- and TMD (*amino acids 1–142*), and TMD (*amino acids 36–142*) GTRAP3-18 (supplemental Fig. S1). The co-transfection of EAAC1 with N and TMD GTRAP3-18 (*lanes 3* and *4*) is unable to reduce the cell surface expression of EAAC1 (*lane 4*). However, the co-transfection of C and TMD (*lanes 5* and *6*) or TMD GTRAP3-18 (*lanes 7* and *8*) is able to reduce the level of complex oligosaccharide EAAC1 (see *arrows*) and the extent of cell surface expression. The membrane expression of EAAC1 is shown for comparison (*lane 2*).

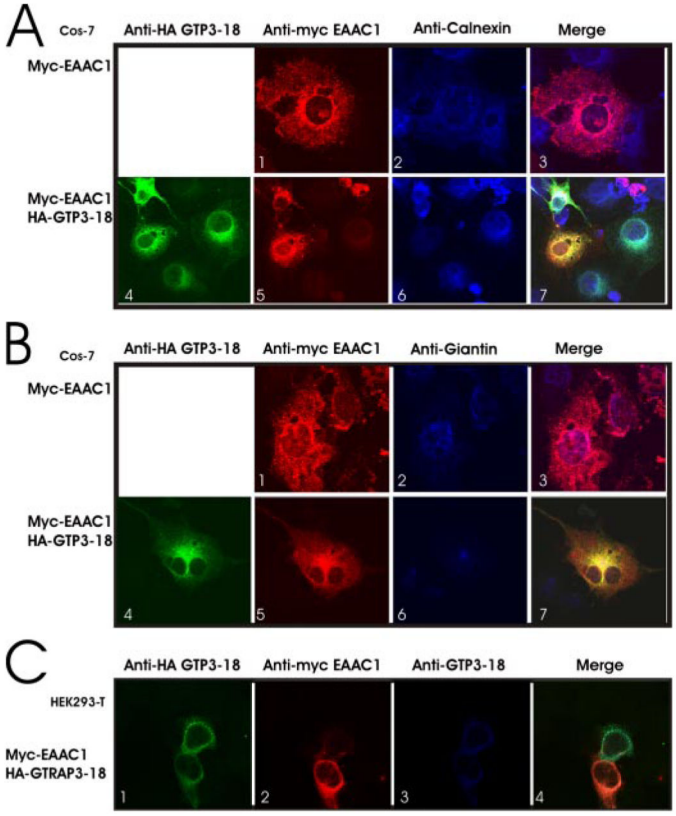

FIGURE 3. GTRAP3-18 is localized to the ER and leads to a redistribution of EAAC1 to the ER

A, EAAC1 (*red*, *panel 1*) has a partial ER residency as defined by co-localization with the integral ER protein, calnexin (*blue*, *panel 2*), and is in multiple endocytic bodies. GTRAP3-18 co-transfection (*green*, *panel 4*) leads to an increase of EAAC1 localized to the ER (*panel 1 versus 5*). *B*, EAAC1 in the Golgi co-localizes with the integral Golgi protein, giantin (*blue*, *panels 2–3*). GTRAP3-18 (*green*, *panel 4*) does not co-localize with giantin (*panel 5*). Following GTRAP3-18 co-expression the relative population of EAAC1 residing in the Golgi is decreased and the reticular appearance of EAAC1 is increased as it co-localizes with GTRAP3-18 (*panels 4–7*). *C*, The HA fusion epitope (*green*, *panel 1*) correlates with GTRAP3-18 polyclonal antibody (*blue*, *panel 3*) immunofluorescence.

Europe PMC Funders Author Manuscripts

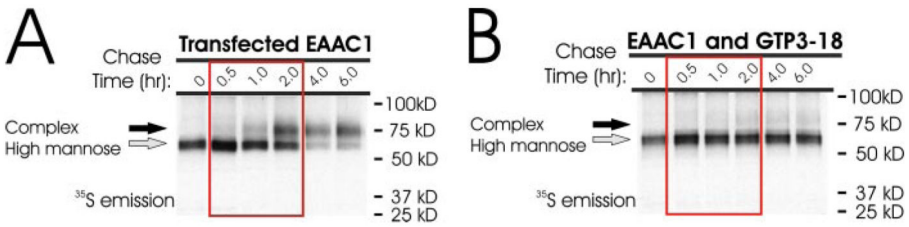

FIGURE 4. GTRAP3-18 delays oligosaccharide maturation of EAAC1 but does not contribute to protein degradation

GTRAP3-18 delays the high mannose to complex oligosaccharide maturation of EAAC1. *A* and *B*, metabolic labeling of EAAC1 by ^{35}S incorporation demonstrates both high mannose and complex oligosaccharide states form within 0.5–1 h (*A*, see *arrows* and *boxed lanes*). Co-transfection with GTRAP3-18 delays the rapid trafficking of EAAC1 to the Golgi thereby preventing the high mannose to complex oligosaccharide transition (*B*, see *arrows* and *boxed lanes*).

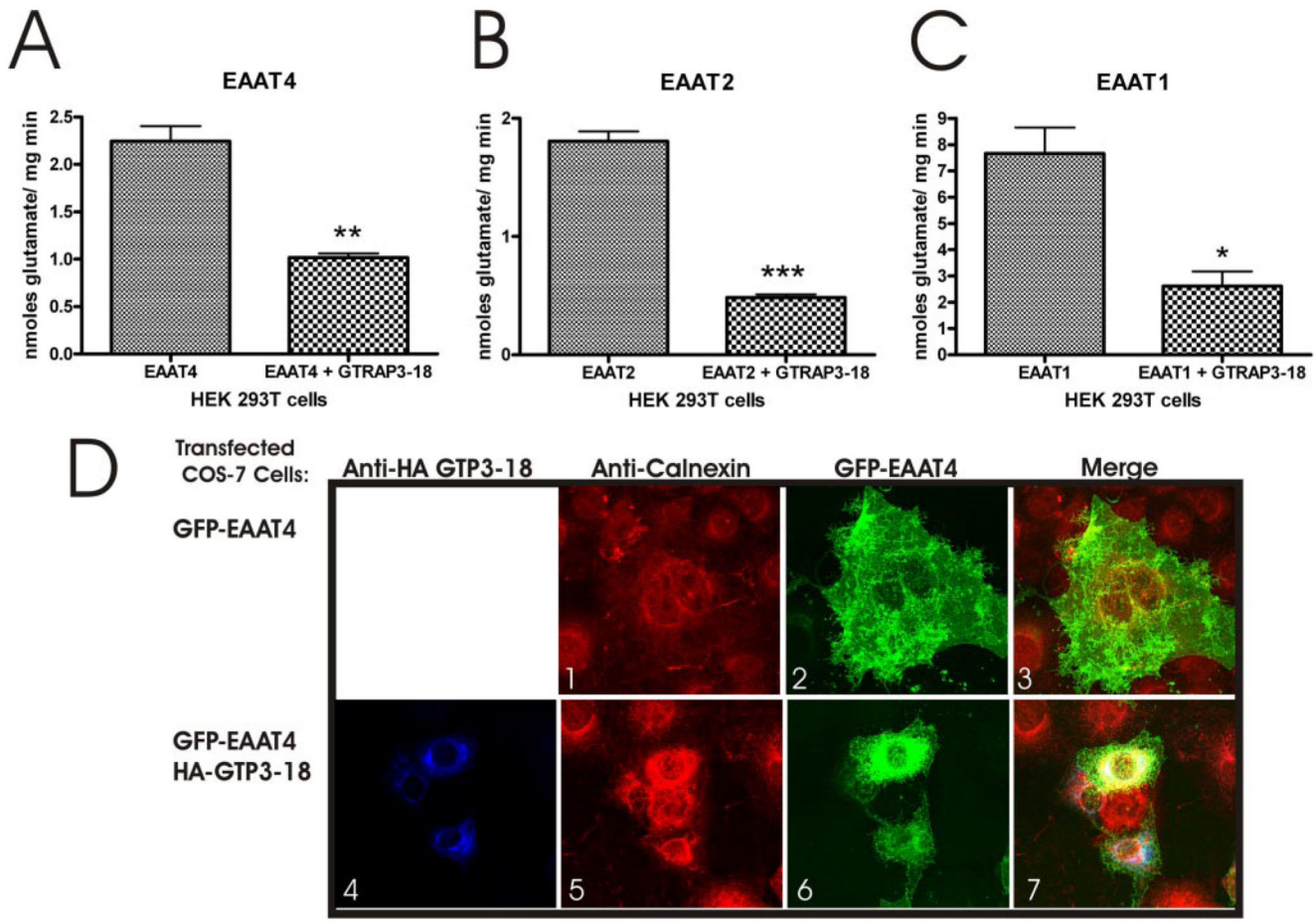

FIGURE 5. GTRAP3-18 reduces the Na^+-dependent glutamate uptake activity of all EAAT isoforms through the delayed acquisition of the complex oligosaccharide state

A–C, activity of the other isoforms in the EAAT family is significantly decreased by equal molar co-transfection with GTRAP3-18, with expression levels of GTRAP3-18 that are low relative to expression of the transporters ($p < 0.01$-0.001). The transporters have some variation in the percent reduction in activity caused by GTRAP3-18; which is related to how well an isoform is trafficked to the surface. The majority of transfected EAAT2 and EAAT4 is localized to the plasma membrane (*5D*) and the reduction caused by GTRAP3-18 is relatively greater than for the isoforms EAAT1 and EAAT3 whose cellular distribution is biased toward intracellular vesicles. *D*, majority of EAAT4 (*green*, *panel 1*) does not localize to the ER (*red*, *panels 2* and *3*). Co-expression with GTRAP3-18 (*blue*, *panel 4*) leads to a redistribution of EAAT4 to the ER (*panels 4–7*). This result is representative of the EAAT family.

Europe PMC Funders Author Manuscripts

TABLE 1

Saturation kinetics analysis of EAAC1 and Glt-1/rEAAT2 following GTRAP3-18 co-transfection in HEK 293 cells

A saturation curve of Na^+-dependent glutamate uptake was performed for each transporter over the range of 0.1–500 μ_M glutamate. EAAC1 and Glt-1/rEAAT2 experienced a 2-fold and a 3-fold reduction, respectively in their mean V_{max} following GTRAP3-18 co-transfection to the similar rates of 5.39 and 5.55 nmol glutamate/mg min ($p < 0.05$).

Transfected cDNA	Mean V_{max}	Mean K_m	p value
		μ_M	
EAAC1	11.41	152.4	$p < 0.05$
EAAC1 and GTRAP3-18	5.393	75.21	
Glt-1/rEAAT2	17.43	211.7	$p < 0.006$
Glt-1/rEAAT2 and GTRAP3-18	5.554	82.24	